Ontogeny of stromal organizer cells during lymph node development

Published in final edited form as:
J Immunol. 2010 April 15; 184(8): 4521–4530. doi:10.4049/jimmunol.0903113.

Ontogeny of Stromal Organizer Cells during Lymph Node Development

Cécile Bénézech[*], **Andrea White**[*], **Emma Mader**[*], **Karine Serre**[*], **Sonia Parnell**[*], **Klaus Pfeffer**[†], **Carl F. Ware**[‡], **Graham Anderson**[*], and **Jorge H. Caamaño**[*]

[*]School of Immunity and Infection, Institute for BioMedical Research-Medical Research Council Centre for Immune Regulation, College of Medical and Dental Sciences, University of Birmingham, Birmingham, United Kingdom

[†]Institut fur Medizinische Mikrobiologie und Krankenhaushygiene, Heinrich-Heine-University, Düsseldorf, Germany

[‡]La Jolla Institute for Allergy and Immunology, La Jolla, CA 92037

Abstract

The development of secondary lymphoid organs, such as lymph nodes (LNs), in the embryo results from the reciprocal action between lymphoid tissue inducer (LTi) cells and stromal cells. However, the initial events inducing LN anlagen formation before the LTi stromal cells cross-talk interactions take place are not fully elucidated. In this study, we show that the inguinal LN anlagen in mouse embryos developed from mesenchymal cells surrounding the lymph sacs, spherical structures of endothelial cells that bud from veins. Using inguinal and mesenteric LNs (mLNs), we provide evidence supporting a two-step maturation model for stromal cells: first, ICAM-1^{-}VCAM-1^{-} mesenchymal precursor cells become ICAM-1^{int}VCAM-1^{int} cells, in a process independent of LTi cells and lymphotoxin β receptor (LTβR) signaling. The second step involves the maturation of ICAM-1^{int}VCAM-1^{int} cells to ICAM-1^{high}VCAM-1^{high} mucosal addressin cell adhesion molecule-1^{+} organizer cells and depends on both LTi cells and LTβR. Addition of αLTβR agonist to LN organ cultures was sufficient to induce ICAM-1^{int}VCAM-1^{int} cells to mature. In *Lt*β*R*$^{-/-}$ embryos, both inguinal and mLN stromal cells showed a block at the ICAM-1^{int}VCAM-1^{int} stage, and, contrary to inguinal LNs, mLNs persist longer and contained LTi cells, which correlated with the sustained gene expression of *Il-7*, C*xcl13*, and, to a lesser degree, *Ccl21*. Taken together, these results highlight the importance of the signals and cellular interactions that induce the maturation of stromal cells and ultimately lead to the formation of lymphoid tissues.

Lymph nodes (LNs) are specialized structures situated at strategic sites in the body along the lymphatic vasculature network. They enable filtration of Ags and pathogens and provide a site for Ag presentation to lymphocytes and induction of adaptive immune responses. LN development is not fully elucidated, although several studies have reported on the role of lymphoid tissue inducer (LTi) cells at late stages of LN formation. Recruitment of LTi cells that express the TNF family molecule lymphotoxin α1β2 to the LN anlagen allows engagement of lymphotoxin β receptor (LTβR)-expressing stromal cells. Subsequently, activation of two

Address correspondence and reprint requests to Dr. Jorge H. Caamaño, IBR-MRC Centre for Immune Regulation, College of Medical and Dental Sciences, University of Birmingham, Birmingham B15 2TT, U.K. j.caamano@bham.ac.uk.

The online version of this article contains supplemental material.

Disclosures
The authors have no financial conflicts of interest.

different pathways of the NF-κB transcription factor results in expression of high levels of ICAM-1, VCAM-1, chemokines, and cytokines by the stromal cells (1–3). However, the early events regulating LN anlagen formation remain unknown.

LN formation is tightly linked to the development of the lymphatic system and in particular to the formation of lymph sacs. Although these events have been described a century ago, our understanding is still limited. In 1902, Sabin (4,5) proposed that lymph sacs form from the budding and sprouting of endothelial cells from veins. In contrast, Huntington and McClure (6) suggested that lymph sacs develop from mesenchymal cells first, before venous endothelial sprouting occurs from the newly formed lymph sacs. More recently, the use of markers specific for lymphatic endothelial cells, such as VEGFR3 (7), Prox-1 (8), and the hyaluronic acid receptor Lyve-1, showed that Lyve-1^{+}Prox-1^{+} endothelial cells located in the anterior cardinal vein bud around embryonic day (E) 10.5–11.5 to form a lymph sac under the guidance of VEGFC signals (9). These data are in agreement with Sabin's model (10), which suggested that stromal cells derive from the lymph sac, which itself has an endothelial origin. Interestingly, a recent report showed that *Prox-1*$^{-/-}$ mouse embryos failed to develop lymph sacs, although they were still able to form primitive LN anlagen, indicating that endothelial cells are not required to form the LN primordium and that the LN anlage derives from distinct cell types (11).

We have previously reported on the isolation of inguinal LN (iLN) anlagen prior to the recruitment of LTi cells (12). In this study, we report on the sequence of events leading to the formation of iLN and mesenteric LN (mLN) anlagen in the mouse embryo. Our observations indicate that iLN anlage develops at the site of interactions between the budding endothelium and surrounding layers of mesenchymal cells that appear to invade the former. Combining confocal microscopy and FACS analysis of E15 iLNs, we show the appearance of the very first stromal cells coexpressing mesenchymal markers, like platelet-derived growth factor receptor (PDGFR)α, and the stromal markers ICAM-1 or gp38/podoplanin. These cells, characterized by their intermediate levels of expression of ICAM-1 and VCAM-1 ($I^{int}V^{int}$), seem to give rise to ICAM-1^{high}VCAM-1^{high} ($I^{high}V^{high}$) mucosal addressin cell adhesion molecule-1 (MAdCAM-$1)^{+}$ stromal organizer cells. This is supported by our findings using an in vitro organ culture system with an agonistic anti-LTβR Ab. The stromal cell maturation correlates with a gradual increase in mRNA levels of cytokine and chemokine genes. We also show that LTβR and LTi cells are required for the $I^{int}V^{int}$ cells to become $I^{high}V^{high}$ organizer cells. Finally, our results demonstrate that in E17 *Lt*β*R*$^{-/-}$ mLN, LTi cells are present and that *Cxcl13*, *Il-7*, and lower levels of *Ccl21* are still expressed, indicating that LTβR is not fully necessary for the initial recruitment of LTi cells to the mLNs.

Our results indicate that lymphoid tissue stromal cells undergo a gradual maturation program to create the proper milieu for recruitment of LTi cells followed by the generation of the specific T and B cell areas in the mature organ.

Materials and Methods

Mice

BALB/c (H-2^{d}), C57BL/6 (H-2^{b}), *Lt*β*R*$^{-/-}$ (H-2^{b}) (13) (C57BL/6 background), and *Ror*γ$^{-/-}$ (H-2^{b}) (14) (C57BL/6 background) mice were bred and maintained under specific pathogen-free conditions in the Biomedical Services Unit at the University of Birmingham (Birmingham, U.K.) according to Home Office and local ethics committee regulations. Day of vaginal plug detection was designated as E0.

Isolation of LN stromal and CD45$^+$ cells and mLN organ culture

iLNs and mLNs were isolated at the indicated embryonic stages by microdissection and were disaggregated by incubation in 2.5 mg/ml collagenase/dispase (R&D Systems, Minneapolis, MN) and 100 μg/ml DNase I (Sigma-Aldrich, St. Louis, MO) in RF10 media at 37°C to obtain single-cell suspensions. In some experiments, freshly isolated mLNs were explanted in fetal organ culture prepared as described (15) and treated with the agonistic anti-LTβR Ab (clone 4H8) at 2 μg/ml for 3 d (16,17).

Abs and flow cytometry

The following Abs were used for flow cytometry: CD45.2-FITC clone 104, ICAM-1–PE clone YN1/1.7.4, VCAM-1–APC clone 429, MAdCAM-1–biotin clone MECA-367, VEGFR-3–biotin clone AFLA4, PDGFR-α–APC clone APA5, (eBioscience, San Diego, CA), and gp38/podoplanin 8.1.1 supernatant (hamster; kind gift from A. Farr, University of Washington, Seattle, WA). Biotinylated Abs were detected using streptavidin-PECy5.5 (eBioscience). gp38/podoplanin Ab was detected using goat anti-hamster– FITC (Southern Biotechnology Associates, Birmingham, AL). All stainings were made in PBS plus 0.1% BSA, 10% mouse serum, and 10% rat serum. Four-color flow cytometric analysis was performed using an FACSCalibur (BD Biosciences, San Jose, CA) with forward/side scatter gates set to exclude nonviable cells. Gates were applied appropriately according to the expression profile of the molecules being assayed. Data were analyzed with FlowJo software (Tree Star, Ashland, OR).

Cell sorting, RT-PCR, real-time RT-PCR

Isolation of the different CD45$^-$ ICAM-1/VCAM-1 mLN stromal cell populations from wild-type (WT) and *Lt*β*R*$^{-/-}$ embryos of the indicated ages was performed by MoFlow (DakoCytomation, Carpinteria, CA) cell sorting from disaggregated LN cell suspensions and then snap frozen for RT-PCR.

High-purity cDNA was generated from purified mRNA using μMacs One-Step cDNA synthesis kit, according to the manufacturer's instructions (Miltenyi Biotec, Auburn, CA). Real-time PCR was performed using IQ SYBR Green Supermix (Bio-Rad, Hercules, CA) with primers specific for β-*actin*, *Ccl21*, *Ccl19*, *Cxcl13*, *Il-7*, *Lt*β*R*, *RelB*, *RankL*, *TnfrI*, and *Mmp9*. PCRs were conducted in triplicate in 10 μl volumes containing 200 nM primers. After an initial denaturation step (95°C for 10 min), cycling was performed at 95°C for 15 s, 60°C for 20 s, and 72°C for 5 s (45 cycles). Specific amplification was verified by melt curve analysis and also by fractionation of PCR products on a 2% agarose gel that were identified by fragment size (data not shown). mRNA transcript levels of each gene were analyzed using Applied Biosystem's SDS software (Applied Biosystems, Foster City, CA) by setting thresholds determining the cycle number at which the threshold was reached (C_t). The C_t of the β-*actin* was subtracted from the C_t of the target gene, and the relative amount was calculated as $2^{-\Delta C_t}$. Means of triplicate reactions (multiply 1000-fold) were represented, and data shown are representative of at least two separate cell-sorting experiments. Primer sequences are shown in Supplemental Fig. 1.

Immunofluorescence stainings

For tissue-section stainings, iLNs and mLNs were isolated and embedded in OCT compound (Tissue Tek, Torrance, CA), then frozen in liquid nitrogen. Six-micrometer sections of tissue were cut and fixed in acetone. Abs used were gp38/podoplanin 8.1.1, ICAM-1–FITC clone YN1/1.7.4, PDGFRα clone APA5, CD44-FITC clone IM7, receptor activator for NF-κB ligand (RANKL)-biotin clone IK22/5, MAdCAM-biotin clone MECA-367 (eBioscience), collagen type I (Chemicon International, Temecula, CA), laminin α5 (rat; gift of A. Zapata, Complutense University, Madrid, Spain) perlecan (rat; gift of Z. Lokmic, Bernard O'Brien Institute of

Microsurgery, Melbourne, Australia), CCL21 (R&DSystems), Lyve-1 (rabbit polyclonal; Abcam, Cambridge, MA), fibronectin clone FN-3E2 (mouse IgM; Sigma-Aldrich), ER-TR7 supernatant (Biogenesis, Poole, U.K.). CD4 was directly conjugated using the Alexa Fluor 647 mAb Labeling Kit (Invitrogen, Carlsbad,CA). ICAM-1–FITC-conjugated Ab was detected using rabbit anti-FITC (Sigma-Aldrich), then goat anti-rabbit IgG-FITC (Jackson ImmunoResearch Laboratories, West Grove, PA). Anti-PDGFRα was detected using anti-rat IgG-Alexa 594 (Molecular Probes, Eugene, OR). Lyve-1 Ab was detected using goat anti-rabbit IgG-FITC (Jackson ImmunoResearch Laboratories). Collagen type I Ab was detected with goat anti-rabbit IgG-biotin (DakoCytomation). CCL21 Ab was detected using donkey anti-goat FITC (Jackson ImmunoResearch Laboratories). gp38/podoplanin and fibronectin Abs were detected using goat anti-hamster biotin (Cambridge Bioscience, Cambridge, U.K.). Biotinylated Abs were detected using streptavidin-Alexa Fluor 555 or 488 (Molecular Probes). Sections were mounted using Vectashield mounting medium (Vector Laboratories, Burlingame, CA).

Image acquisition and analysis of confocal images

For tissue-section stainings, confocal images were acquired using a Zeiss LSM 510 laser scanning confocal head with a Zeiss Axio Imager Z1 microscope (Zeiss, Oberkochen, Germany). Digital images were recorded in four separately scanned channels with no overlap in detection of emissions from the respective fluorochromes. Confocal micrographs were stored as digital arrays of 2048 × 2048 pixels with 8-bit sensitivity; detectors were routinely set so that intensities in each channel spanned the 0–255 scale optimally.

Results

Inguinal LN anlagen formed by budding endothelial cells surrounded by mesenchymal cells

Over the past few years, the structure of the developing LN anlagen in the mouse embryo had been studied by assessing the recruitment and presence of LTi cells in sections of whole mouse embryos (11,18–20). However, the iLN anlage forms a very distinct structure that can be dissected as early as E13. Our previous studies have shown that E15 iLNs contain very few $CD45^+$ cells and no $CD4^+IL7R\alpha^+$ LTi cells (12). Therefore, experimental approaches relying on the presence of LTi cells for the identification of LN anlagen do not allow for early detection and analysis of LN primordium. For an in-depth analysis of LN anlage development prior to LTi cell colonization, we examined sections of dissected E13 and E15 iLNs.

At E13, the primitive iLN anlage had a spherical shape formed by a bud of tightly packed gp38/$podoplanin^+$ cells surrounded by layers of fibroblast-like cells that expressed the component of the reticular network ER-TR7 (Fig. 1*A*). We further characterized these two cellular compartments for the expression of endothelial and mesenchymal markers on E15 iLNs sections by immunofluorescence staining and confocal imaging.

The bud of gp38/$podoplanin^+$ cells expressed the endothelial markers ICAM-1 and CCL21 and the extracellular matrix proteins collagen type I, and laminin α5 (Fig. 1*B*, *left columns*). Perlecan staining was restricted to a thin layer at the interface between the endothelial and the mesenchymal cells, indicating the presence of an intact basement membrane produced by the former.

The fibroblast-like cells that formed the outer layers of the LN primordium expressed several molecules characteristic of mesenchymal cells, such as PDGFRα, the extracellular matrix protein fibronectin, ER-TR7, and the hyaluronic acid receptor CD44 (Fig. 1*B*, *right columns*).

Staining of iLN sections demonstrated that ER-TR7$^+$ stromal cells and the gp38/podoplanin$^+$ lymphatic endothelial cell compartment remained separated up to E16, and then ER-TR7$^+$ cells appeared to invade the endothelial core to form the proper internal compartments of the anlage (Fig. 2, Supplemental Fig. 2). Following that process, a large number of mesenchymal cells at E17 expressed both ER-TR7 and gp38/podoplanin and could be distinguished from the single-positive cells (Supplemental Fig. 2).

Based on the above observations, we envision the structure of the E13–15 iLN anlagen comprising two distinct cells types, a bud of lymphatic endothelial cells forming the lymph sacs, surrounded by a basement membrane and layers of mesenchymal cells.

Ongoing remodeling of the iLN anlage structure between E15 and E17

To further define the organ remodeling taking place between E15 and E17 in iLNs, we tracked the changes occurring in the mesenchymal and endothelial compartments by analyzing E17 iLNs, when LTi cells arrived to the anlagen. Immunofluorescence staining of molecules expressed in endothelial and mesenchymal cells were performed in E17 iLN sections and compared with the stainings of these organs at E15.

The endothelial cells that formed a central bud at E15 still form the core of the anlagen at E17 (Fig 2, circled by a white line), but now contained perlecan$^+$ laminin α5$^+$ structures that form the LN vasculature (Fig. 2*A*, 2*D*).

The mesenchymal cells formed the outer structure of the LN anlage, similar to what was observed at E15. However, at E17, mesenchymal cells expressing fibronectin and PDGFRα started to migrate to the endothelial core, as shown in the central region delimitating the endothelium (Fig. 2*C–H*). CD44 staining (Fig. 2*I*) highlighted the structure of the mesenchymal compartment as well as hematopoietic cells (round cells) that have entered the LN anlagen. Fibronectin also started to be expressed by cells of the vasculature (Fig. 2*C*, 2*E*, arrowheads). Taken together, these observations show the dynamic changes occurring between E15 and E17 in the iLN anlagen involving both the endothelium and the mesenchyme. For the endothelium, the most dramatic change consisted of the remodeling of the whole vasculature and for the mesenchyme of the invasion of the central endothelial compartment. We further characterize the endothelial and mesenchymal cell populations to better understand their contribution to LN anlagen formation.

Concomitant emergence of stromal organizer cells during remodeling of the iLN structure

The LN organizer cells have been previously characterized by their coexpression of ICAM-1 and VCAM-1 on mLNs, and the stainings suggested a differentiation of the organizer cells from mesenchymal cells (18,21,22). We assessed by FACS analysis the presence of these cells at different stages of embryonic iLN development. At E15, we were able to clearly identify the mesenchymal and endothelial cell compartments described in Fig. 1: 1) the mesenchymal cell precursors that were negative for ICAM-1 andVCAM-1(I$^-$V$^-$) and PDGFRα$^+$ that correlated with the fibroblast-like cells of the surrounding mesenchyme in Fig. 1*B*; and 2) the ICAM-1 singlepositive (I$^+$V$^-$) endothelial cells that also expressed gp38/podoplanin and MAdCAM-1 and were VEGFR3$^-$, similar to the central endothelium shown in Fig. 1*B* (Fig. 3*A*, *top panels*). Interestingly, we identified a third cell population that expressed intermediate levels of ICAM-1 and VCAM-1 (I^{int}V^{int}) that were PDGFRα$^+$ and gp38/podoplanin$^+$, suggesting that they derived from the I$^-$V$^-$ mesenchymal cells. At E17, the mature stromal organizer cells were identified by their high expression of ICAM-1 and VCAM-1 (I^{high}V^{high}) as well as MAdCAM-1, a late differentiation marker. Mature organizer cells also expressed PDGFRα and gp38/podoplanin but not VEGFR3, suggesting that their progenitors were the I^{int}V^{int} cell population.

The I^+V^- endothelial cell population was negative for both VEGFR-3 and the lymphatic marker Lyve-1 at E15 but became positive for both molecules at E17, indicating an ongoing differentiation process toward lymphatic endothelial cells (Fig. 3*A*, *bottom panels*, and data not shown). These results indicate that mesenchymal cells start to mature before the lymphatic endothelium is fully differentiated.

To summarize, vascular/lymphatic endothelial cells could be defined as I^{+V-} gp38/podoplanin$^+$ VEGFR3$^+$ PDGFRα^-, whereas the mesenchymal cell compartment encompassed the I^-V^-, $I^{int}V^{int}$, and $I^{high}V^{high}$ MAdCAM-1$^+$ gp38/podoplanin$^+$ PDGFRα^+ VEGFR3$^-$ cells.

Stromal cells of the iLN and mLN followed a similar pattern of development

Blocking of LTβR in pregnant female mice has shown that mLNs are the first to develop in the embryos and are followed by formation of LNs from head to tail (1,23,24). Several reports have indicated the different developmental requirements for mLN and iLN formation (25–27). A recent report has also shown differences in the stromal cell subsets in these organs in newborn mice (18), and we wanted to investigate whether those differences were already present in embryos and whether mLN stromal cells expressed similar molecules than their iLN counterparts. Indeed, E15 mLN showed an increased frequency of the $I^{int}V^{int}$ cell population, explained by the earlier development of the mLN anlage compared with iLN. However, the same three compartments were still identifiable: 1) mesenchymal cells that were I^-V^-; 2) $I^{int}V^{int}$ cells; and 3) I^+V^- endothelial cells that also expressed MAdCAM-1 (Fig. 2*B*, *top panel*). At E17, the mature stromal organizer cells $I^{high}V^{high}$ were present expressing MAdCAM-1, as well as the I^-V^- mesenchymal and the $I^{int}V^{int}$ cells. However, the I^+V^- endothelial cells were not clearly identifiable in the mLNs at this stage (Fig. 3*B*).

Cellular localization and expression of different molecules were assessed by immunofluorescence staining in E18 iLNs and mLNs. Both organs showed the presence of CD4$^+$IL-7Rα^+ LTi cells as well as stromal organizer cells that expressed RANKL and MAdCAM-1 (Fig. 4). Some lymphatic endothelial cells in the developing subcapsular sinus surrounding the E18 mLNs and iLNs coexpressed MAdCAM-1 and Lyve-1, showing no difference in the presence and structure of the lymphatic endothelium between iLN and mLN (Fig. 4, *middle panels*). Thus, the absence of an I^+V^- endothelial cell population in E17 mLNs compared with iLNs might be due to the stripping of the mLN capsule during dissection of the organs prior to FACS analysis (Fig. 3*A*, 3*B*).

Gradient of gene expression of stromal organizer markers during maturation of the mesenchyme

To confirm the sequence of maturation of the mesenchyme, we assessed the mRNA levels of several genes that are characteristic of stromal cells. The small number of cells present in embryonic iLNs prevented a more in-depth analysis. To have a significant number of stromal cells for these assays, CD45$^-$ cell populations (I^-V^-, $I^{int}V^{int}$, and $I^{high}V^{high}$) were isolated from E18 mLNs, and the gene expression profile was analyzed by quantitative PCR (qPCR).

The expression of most of the genes analyzed was nil in I^-V^- cells with the exception of *Tnf-R1* and *Ccl21*. All CD45$^-$ cells expressed *Lt*β*R*, but only the differentiating $I^{int}V^{int}$ and $I^{high}V^{high}$ cells expressed *RelB*. The $I^{high}V^{high}$ stromal organizer cells expressed the highest levels of homeostatic chemokines (*Ccl21*, *Ccl19*, and *Cxcl13*) (18), *RankL* and *Il-7*, confirming their potential to attract and stimulate LTi cells (Fig. 5). The $I^{int}V^{int}$ and $I^{high}V^{high}$ cells expressed *Mmp9*, which has been shown to increase cellular invasiveness and mobility, indicating a role in tissue remodeling by these cell subsets. Finally, we noticed that all the markers studied showed a gradient of expression, with the $I^{high}V^{high}$ cells showing the highest

levels, followed by $I^{int}V^{int}$ and $I^{-}V^{-}$ that reflected the stage of maturation of the stroma (Fig. 5).

Absence of LtβR or LTi cells resulted in a block of stromal cell maturation at the $I^{int}V^{int}$ stage

LN development is strictly dependent on LTi cells and LTβR signaling, as adult *Rorγ*$^{-/-}$, *LtβR*$^{-/-}$, and *Ltα*$^{-/-}$ mice lack all LNs (13,14,26,28,29). We assessed whether LTβR signaling and LTi cells were required for the initial step of stromal cell maturation or for full progression of these cells to the $I^{high}V^{high}$ stage. FACS analysis of stromal cell populations from E15 iLN and mLN anlagen from WT, *LtβR*$^{-/-}$, and *Rorγ* $^{-/-}$ embryos showed the emergence of the $I^{int}V^{int}$ cells in all strains (Fig. 6*A*). However, at E17, the iLNs were difficult to find in both *LtβR*$^{-/-}$ and *Rorγ*$^{-/-}$ embryos, and what remained had the appearance of fibrous structures (data not shown). FACS analysis of the few iLNs isolated from these mutants confirmed the absence of the $I^{high}V^{high}$ mature stromal organizer cells in both strains (Fig. 6*A*).

We next investigated whether mLNs were similarly affected in their development as iLNs in these mutants. In contrast to the low numbers of iLNs found in E17 *LtβR*$^{-/-}$ or *Rorγ* $^{-/-}$ mice, mLNs were present in normal numbers in embryos from these strains. However, FACS analysis of stromal cells revealed a similar block on the progression from $I^{int}V^{int}$ to $I^{high}V^{high}$ mature organizer cells (Fig. 6*A*).

Recruitment of $CD45^{+}$ cells to iLNs and mLNs between E15 and E17 was impaired in *LtβR*$^{-/-}$ and *Rorγ*$^{-/-}$ embryos. For example, in WT iLNs, we observed an 18-fold increase in the recruitment of $CD45^{+}$ cells between E15 and E17 and only a 1.6- and a 6-fold increase in iLNs from *LtβR*$^{-/-}$ and *Rorγ*$^{-/-}$ embryos, respectively (Fig. 6*A*).

Our analyses showed that LTβR engagement and the presence of LTi cells were required for the appearance of the $I^{high}V^{high}$ mature organizer cells but not for progression of mesenchymal cells from $I^{-}V^{-}$ toward the $I^{int}V^{int}$ compartment.

LTβR-induced maturation of stromal cells from $I^{int}V^{int}$ to $I^{high}V^{high}$

We next tested whether the $I^{int}V^{int}$ stromal cells were the precursors of the $I^{high}V^{high}$ organizer cells. E14 mLNs and E15 iLNs were stimulated in organ cultures with an agonistic αLTβR Ab and the ICAM-1 and VCAM-1 expression profiles of the $CD45^{-}$ cell populations were assessed by FACS analysis. As shown in Fig. 6*B*, a significant increase in the frequency of $I^{high}V^{high}$ cells was detected. Of note, E14 mLNs and E15 iLNs contained very few if any $I^{high}V^{high}$ cells, suggesting that LTβR stimulation induced either those few cells to proliferate or the $I^{int}V^{int}$ cells to mature, becoming $I^{high}V^{high}$ organizer cells. Cell counts prior to and after LTβR stimulation in organ cultures demonstrated no increase in cell numbers (data not shown). These results strongly suggest that the $I^{int}V^{int}$ cell population gives origin to $I^{high}V^{high}$ organizer cells and that signaling through the LTβR was necessary and sufficient to induce the maturation.

LTβR is not fully required for the recruitment retention of LTi cells to mLNs

The accumulation of LTi cells in the LN anlagen may result from active recruitment of these cells or proliferation of LTi cells or their precursors. A previous report showed that proliferation of hematopoietic cells was very rare in LN anlagen, indicating that recruitment of LTi cells and their precursors might be the dominant mechanism (19). IL-7Rα and CXCL13 (ligand of CXCR5 expressed by LTi cells) have been shown to play an important role in the recruitment of LTi cells, and IL-7 is thought to be an early localization signal, as late blockade of this cytokine had minor effects on LTi cell migration and LN development (19).

Cell sorting of mLN cells from E15 WT and *LtβR*$^{-/-}$ embryos and qPCR were used to assess the effect of LTβR deficiency in stromal cell production of chemokines and survival factors

for LTi cells. *Cxcl13* and *Il-7* were expressed at similar levels by the $I^{int}V^{int}$ cells in both WT and *Ltβ*$R^{-/-}$ cells. We also noted that *Ccl21* was mainly expressed by the $I^{+}V^{-}$ endothelial cells, and its expression was reduced but still present in *Ltβ*$R^{-/-}$ E15 mLN cells (Fig. 7*A*) (2).

The presence of LTi cells was assessed in E17 iLNs and mLNs from WT and *Ltβ*$R^{-/-}$ embryos. A very low percentage of both $CD45^{+}$ cells and LTi cells was present in *Ltβ*$R^{-/-}$ iLNs when compared with WT (Fig. 7*B*). Interestingly, whereas the percentage of $CD45^{+}$ cells was reduced in *Ltβ*$R^{-/-}$ compared with WT E17 mLNs, a similar frequency of LTi cells was found in both strains, corroborating previous findings in E16.5 *Ltα*$^{-/-}$ embryos (19). Staining of sections of E16 mLNs from WT and *Ltβ*$R^{-/-}$ embryos confirmed the presence of LTi cells in both strains and showed a significant reduction in MAdCAM-1 and undetectable levels of RANKL in the latter (Fig. 7*C*).

These results showed that although overall colonization by $CD45^{+}$ cells is reduced in the mLNs of *Ltβ*$R^{-/-}$ embryos, LTi cells are still being recruited, suggesting that LTβR signals are not fully required. However, MAdCAM-1 and RANKL levels are severely reduced in these organs, showing their dependence on the LTβR pathway. Based on the results shown above we propose a specific role for LTβR signaling in stromal cells during maturation (Fig. 8, see *Discussion*).

Discussion

The majority of LN development studies have used whole mount sections of mouse embryos and relied on the accumulation of LTi cells for the identification of LN primordium (11,18–20). Therefore, little is known about the initiating events that take place before the recruitment/arrival of LTi cells to the LN anlage. We took advantage of the well-defined structure of the early iLN and performed microdissection of intact anlage to show that the LN primordium developed where endothelial cells formed a spherical body, the lymph sac. This endothelium is surrounded by a $perlecan^{+}$ basement membrane and expressed gp38/podoplanin, ICAM-1, and CCL21. Expression of Lyve-1 and VEGFR3 was not detected by immunofluorescence staining at E13 and appeared around E17 indicating an undergoing differentiation process toward lymphatic phenotype. Based on these observations, we confirmed Sabin's findings (4,5) using pig embryos in that LN anlagen formed at sites of endothelial cell budding from veins to form the primitive lymph sacs.

We showed that layers of mesenchymal cells surround the iLN endothelial bud and that mesenchyme and endothelium remained two distinct compartments until E17, when mesenchymal cells started to invade the former. Remodeling of the iLN anlage is concomitant with the differentiation of the lymphatic endothelium and the recruitment of LTi cells that induce the maturation of stromal cells to become proper organizer cells. Therefore, all these essential milestones of iLN organogenesis appear to take place in a short length of time. The signals that induce the mesenchymal cells to degrade the basement membrane and invade the lymph sacs and whether endothelial-mesenchymal cell cross-talk interactions are important for this process and for the differentiation of the lymphatic endothelium remain to be investigated.

To understand the maturation process of the mesenchymal cell populations and their contribution to the formation of the LN anlagen stroma, we tracked the emergence of the $I^{high}V^{high}$ mature organizer cells by FACS analyses. E15 iLNs, that appear to lack LTi cells, do contain $I^{int}V^{int}PDGFR\alpha^{+}$ cells suggesting that the latter are derived from the $PDGFR\alpha^{+}$ mesenchymal cell layers that surround the lymph sacs. In this regard, a recent report has shown that lymph sacs are not required for the initiation of LN anlagen development (11), suggesting that stromal cell differentiation does not depend on the endothelium and can take place in its absence. In addition, we suggest that the $I^{int}V^{int}$ gp38/$podoplanin^{+}$ cell population will give

rise to the mature $I^{high}V^{high}$ MAdCAM-1^+ stromal organizer cells. The common expression of PDGFRα by I^-V^-, $I^{int}V^{int}$, and $I^{high}V^{high}$ cells and gp38/podoplanin by $I^{int}V^{int}$ and $I^{high}V^{high}$ cells but not VEGFR3 suggested a precursor-product relationship between them. iLN and mLN anlagen develop at different times during embryogenesis, have different developmental requirement, and contain different frequencies of $I^{int}V^{int}$ stromal cells. As shown before in newborn mice, embryonic mLNs have a higher percentage of $I^{int}V^{int}$ stromal cells than iLNs but that does not reflect in a larger proportion of $I^{high}V^{high}$ organizer cells because the latter is lower in mLNs than iLNs (Fig. 3*A*, 3*B*,Fig. 6*A*) (18). However, the sequence of stromal cell maturation is similar in both LNs.

Although several reports had demonstrated that LN development is strictly dependent on LTi cells and LTβR signaling as adult *Rorγ*$^{-/-}$, *LtβR*$^{-/-}$, and *Ltα*$^{-/-}$ mice lack most LNs, the fate of the developing LN anlagen in those mutants had not been characterized (13,14,26,28,29). Other groups and ours (11,12,19) have indicated that two different signals are required for stromal organizer cell maturation. We have shown previously that in the absence of lymphotoxin α and hence lymphotoxin α1β2, the maturation of stromal cells was blocked at the $I^{int}V^{int}$ stage (12). However, a role for LTβR engagement by ligands other than lymphotoxin α1β2 to induce the transition of I^-V^- mesenchymal cells to the $I^{int}V^{int}$ stage could not be ruled out. Analysis of the *LtβR*$^{-/-}$ LNs showed that this receptor does not have a role in the first step of stromal cell maturation. Thus, the signal(s) for the initial step of stromal cell maturation remains elusive. Lymphotoxin α and LTβR engagement and the presence of LTi cells were required for the second step of this process, for *LtβR*$^{-/-}$ and *Rorγ*$^{-/-}$ mouse embryos showed normal development of iLNs and mLNs up to E15 but stromal cell maturation did not progress further than the $I^{int}V^{int}$ stage, and iLNs quickly regressed. Stimulation of E14 mLNs through LTβR induced a strong increase in the frequency of $I^{high}V^{high}$ MAdCAM-1^+ stromal organizer cells that seems to be independent of cell proliferation. Similar results were obtained upon LTβR stimulation of E15 iLNs, although upregulation of MAdCAM-1 expression was lower than in mLN stromal cells. Taken together, these results support the hypothesis of a precursor-product relationship between the $I^{int}V^{int}$ cells and the $I^{high}V^{high}$ MAdCAM-1^+ stromal organizer cells.

We investigated the gene expression profile of three $CD45^-$ cell populations from E18 mLNs, I^-V^-, $I^{int}V^{int}$, and $I^{high}V^{high}$. Our results showed that although I^-V^- mesenchymal precursors cells expressed *Ltβ*R mRNA, one of its downstream effectors, the transcription factor *Relb*, was expressed only in the maturing $I^{int}V^{int}$ and $I^{high}V^{high}$ cells. This finding suggests that the first step of stromal cell maturation enables the LN anlagen to respond to LTβR signaling by inducing the expression of the downstream proteins of this cascade. In agreement with this, *RankL* was expressed at 1000-fold higher levels in the $I^{high}V^{high}$ cell population than in the $I^{int}V^{int}$ cells. Concomitantly, mLNs from E16.5 *Ltβ*R-deficient embryos, whose stromal cells are blocked at the $I^{int}V^{int}$ cell stage, showed no expression of RANKL. In contrast, *Ccl21*, *Cxcl13*, and *Il*-7 were expressed in both $I^{int}V^{int}$ and $I^{high}V^{high}$ cell populations, indicating that these genes are less dependent on LTβR engagement for their full expression. In agreement with this, the mRNA levels of *Cxcl13* and *Il*-7 were not decreased in E15 mLN of *Ltβ*R-deficient embryos. *Ccl21* expression was significantly decreased in endothelial cells correlating with previous reports on the expression of CCL21 by endothelial cells of high endothelial venules and the role of LTβR–NF-κB2 in the latter (30–34). These results are in agreement with the findings of Moyron-Quiroz and colleagues (35) showing that CXCL13 and CCL21 were expressed independently of lymphotoxin α during the formation of inducible bronchial-associated lymphoid tissues. A recent report has indicated that retinoic acid expressed by neurons induces the expression of *Cxcl13* in LN anlagen independently of LTβR signaling (36).

At E17 when iLNs from *Ltβ*$R^{-/-}$ mice have regressed, mLNs were still present in this mutant but showed a failure to induce RANKL and MAdCAM-1 in stromal cells compared with WT mLNs, highlighting the importance of LTβR signaling for the expression of these molecules (20). The absence of RANKL expression in the *Ltβ*$R^{-/-}$ mLN may compromise the survival of LTi cells, which may be dependent on RANK signaling, as suggested by the reduced number of these cells found in the mLNs of newborn mice deficient in this pathway or the intracellular adaptor TNFR-associated factor-6 as well as in embryos treated with RANK-Ig fusion protein (19,37,38). These findings correlate with the fact that rudimentary mLNs have been found in newborn *Ltβ*$R^{-/-}$ mice.

Based on the results shown in this study, we propose a two-step stromal cell maturation model (Fig. 8). First, the I^-V^- mesenchymal cells are primed by a yet unknown signal to give rise to an $I^{int}V^{int}$ gp38/podoplanin$^+$ cell population, able to recruit LTi cells by their expression of *Il-7*, *Ccl21*, and *Cxcl13* and to respond to LTβR engagement via acquisition of the expression of RelB. Second, the $I^{int}V^{int}$ cells gave rise to the mature $I^{high}V^{high}$ MAdCAM-1$^+$ stromal organizer cells. Following these essential maturation steps during embryogenesis, LN stromal cells require stimulation by IL-7Rα$^+$ cells at the time of birth to sustain LN development and organization (39).

It is clear that stromal cell function in lymphoid tissues is more than contributing a support for the exquisite architecture of these organs. Stromal cells also have a role in B and T cell homeostasis as well as in the organization of specific cell areas to facilitate the localization and interaction of cells during immune responses (40,41). All these functions suggest the existence of different subsets of stromal cells, and further studies will be necessary to investigate the ontogeny of fibroblastic reticular cells and marginal reticular cells (42–45). We are currently investigating the origin of the I^-V^- mesenchymal cell precursors, the signals that induce priming on those cells to become $I^{int}V^{int}$ and the role for the recently described lymphoid tissue initiator cells have in this process (46).

The process of maturation of lymphoid tissue stromal cells might have similarities with the recently described changes in the stromal microenvironment resulting in the differentiation of lymphoid stromal cells during the formation of ectopic lymphoid tissues (47).

Supplementary Material

Refer to Web version on PubMed Central for supplementary material.

Acknowledgments

We thank the personnel in Biomedical Services Unit for taking good care of our animal colonies; Eric Jenkinson for continuing support; and the Anderson and Lane Laboratories, Elodie Mohr, Guillaume Desanti, and Dave Withers for helpful discussions and comments on the manuscript. We also thank Dan Littman and Daniela Finke for providing the *Rorγ*$^{-/-}$ mice and Roger Bird for cell sorting.

This work was supported by a Biotechnology and Biological Sciences Research Council project grant (to J.H.C. and G.A). Work in the laboratory of C.F.W. was supported by National Institutes of Health Grant AI33068. E.M. is the recipient of a Medical Research Council Doctoral Training Account Ph.D. studentship.

Abbreviations used in this paper

C_t	cycle threshold
E	embryonic day
iLN	inguinal lymph node

$I^{-}V^{-}$	negative for ICAM-1 and VCAM-1
$I^{+}V^{-}$	ICAM-1 single-positive
$I^{high}V^{high}$	high expression of ICAM-1 and VCAM-1
$I^{int}V^{int}$	intermediate levels of ICAM-1 and VCAM-1
LN	lymph node
LTβR	lymphotoxin β receptor
LTi	lymphoid tissue inducer
MAdCAM-1	mucosal addressin cell adhesion molecule-1
mLN	mesenteric lymph node
NA	numerical aperture
PDGFR	platelet-derived growth factor receptor
qPCR	quantitative PCR
RANKL	receptor activator for NF-κB ligand
WT	wild-type

References

1. Mebius RE. Organogenesis of lymphoid tissues. Nat. Rev. Immunol 2003;3:292–303. [PubMed: 12669020]
2. Randall TD, Carragher DM, Rangel-Moreno J. Development of secondary lymphoid organs. Annu. Rev. Immunol 2008;26:627–650. [PubMed: 18370924]
3. Ruddle NH, Akirav EM. Secondary lymphoid organs: responding to genetic and environmental cues in ontogeny and the immune response. J. Immunol 2009;183:2205–2212. [PubMed: 19661265]
4. Sabin F. On the origin of the lymphatic system from the veins and the development of the lymph hearts and thoracic in the pig. Am. J. Anat 1902;1:367–389.
5. Sabin F. The lymphatic system in human embryos, with a consideration of the morphology of the system as a whole. Am. J. Anat 1909;1:43–91.
6. Huntington G, McClure C. The anatomy and development of the jugular lymph sac in the domestic cat (Felis domestica). Am. J. Anat 1910;10:177–311.
7. Kaipainen A, Korhonen J, Mustonen T, van Hinsbergh VW, Fang GH, Dumont D, Breitman M, Alitalo K. Expression of the fms-like tyrosine kinase 4 gene becomes restricted to lymphatic endothelium during development. Proc. Natl. Acad. Sci. U.S.A 1995;92:3566–3570. [PubMed: 7724599]
8. Wigle JT, Oliver G. Prox1 function is required for the development of the murine lymphatic system. Cell 1999;98:769–778. [PubMed: 10499794]
9. Karkkainen MJ, Haiko P, Sainio K, Partanen J, Taipale J, Petrova TV, Jeltsch M, Jackson DG, Talikka M, Rauvala H, et al. Vascular endothelial growth factor C is required for sprouting of the first lymphatic vessels from embryonic veins. Nat. Immunol 2004;5:74–80. [PubMed: 14634646]
10. Oliver G, Alitalo K. The lymphatic vasculature: recent progress and paradigms. Annu. Rev. Cell Dev. Biol 2005;21:457–483. [PubMed: 16212503]
11. Vondenhoff MF, van de Pavert SA, Dillard ME, Greuter M, Goverse G, Oliver G, Mebius RE. Lymph sacs are not required for the initiation of lymph node formation. Development 2009;136:29–34. [PubMed: 19060331]
12. White A, Carragher D, Parnell S, Msaki A, Perkins N, Lane P, Jenkinson E, Anderson G, Caamaño JH. Lymphotoxin a-dependent and -independent signals regulate stromal organizer cell homeostasis during lymph node organogenesis. Blood 2007;110:1950–1959. [PubMed: 17526859]

13. Fütterer A, Mink K, Luz A, Kosco-Vilbois MH, Pfeffer K. The lymphotoxin beta receptor controls organogenesis and affinity maturation in peripheral lymphoid tissues. Immunity 1998;9:59–70. [PubMed: 9697836]
14. Sun Z, Unutmaz D, Zou YR, Sunshine MJ, Pierani A, Brenner-Morton S, Mebius RE, Littman DR. Requirement for RORgamma in thymocyte survival and lymphoid organ development. Science 2000;288:2369–2373. [PubMed: 10875923]
15. Anderson G, Partington KM, Jenkinson EJ. Differential effects of peptide diversity and stromal cell type in positive and negative selection in the thymus. J. Immunol 1998;161:6599–6603. [PubMed: 9862687]
16. Browning JL, Dougas I, Ngam-ek A, Bourdon PR, Ehrenfels BN, Miatkowski K, Zafari M, Yampaglia AM, Lawton P, Meier W, et al. Characterization of surface lymphotoxin forms. Use of specific monoclonal antibodies and soluble receptors. J. Immunol 1995;154:33–46. [PubMed: 7995952]
17. Dejardin E, Droin NM, Delhase M, Haas E, Cao Y, Makris C, Li ZW, Karin M, Ware CF, Green DR. The lymphotoxin-beta receptor induces different patterns of gene expression via two NF-kappaB pathways. Immunity 2002;17:525–535. [PubMed: 12387745]
18. Cupedo T, Vondenhoff MF, Heeregrave EJ, De Weerd AE, Jansen W, Jackson DG, Kraal G, Mebius RE. Presumptive lymph node organizers are differentially represented in developing mesenteric and peripheral nodes. J. Immunol 2004;173:2968–2975. [PubMed: 15322155]
19. Eberl G, Marmon S, Sunshine MJ, Rennert PD, Choi Y, Littman DR. An essential function for the nuclear receptor RORgamma(t) in the generation of fetal lymphoid tissue inducer cells. Nat. Immunol 2004;5:64–73. [PubMed: 14691482]
20. Vondenhoff MF, Greuter M, Goverse G, Elewaut D, Dewint P, Ware CF, Hoorweg K, Kraal G, Mebius RE. LTbetaR signaling induces cytokine expression and up-regulates lymphangiogenic factors in lymph node anlagen. J. Immunol 2009;182:5439–5445. [PubMed: 19380791]
21. Nishikawa S, Honda K, Vieira P, Yoshida H. Organogenesis of peripheral lymphoid organs. Immunol. Rev 2003;195:72–80. [PubMed: 12969311]
22. Okuda M, Togawa A, Wada H, Nishikawa S. Distinct activities of stromal cells involved in the organogenesis of lymph nodes and Peyer's patches. J. Immunol 2007;179:804–811. [PubMed: 17617570]
23. Rennert PD, Browning JL, Mebius R, Mackay F, Hochman PS. Surface lymphotoxin alpha/beta complex is required for the development of peripheral lymphoid organs. J. Exp. Med 1996;184:1999–2006. [PubMed: 8920886]
24. Rennert PD, James D, Mackay F, Browning JL, Hochman PS. Lymph node genesis is induced by signaling through the lymphotoxin beta receptor. Immunity 1998;9:71–79. [PubMed: 9697837]
25. Banks TA, Rouse BT, Kerley MK, Blair PJ, Godfrey VL, Kuklin NA, Bouley DM, Thomas J, Kanangat S, Mucenski ML. Lymphotoxin-alpha-deficient mice. Effects on secondary lymphoid organ development and humoral immune responsiveness. J. Immunol 1995;155:1685–1693. [PubMed: 7636227]
26. Koni PA, Sacca R, Lawton P, Browning JL, Ruddle NH, Flavell RA. Distinct roles in lymphoid organogenesis for lymphotoxins alpha and beta revealed in lymphotoxin beta-deficient mice. Immunity 1997;6:491–500. [PubMed: 9133428]
27. Scheu S, Alferink J, Pötzel T, Barchet W, Kalinke U, Pfeffer K. Targeted disruption of LIGHT causes defects in costimulatory T cell activation and reveals cooperation with lymphotoxin beta in mesenteric lymph node genesis. J. Exp. Med 2002;195:1613–1624. [PubMed: 12070288]
28. Cook MC, Körner H, Riminton DS, Lemckert FA, Hasbold J, Amesbury M, Hodgkin PD, Cyster JG, Sedgwick JD, Basten A. Generation of splenic follicular structure and B cell movement in tumor necrosis factor-deficient mice. J. Exp. Med 1998;188:1503–1510. [PubMed: 9782127]
29. Eberl G, Littman DR. The role of the nuclear hormone receptor RORgammat in the development of lymph nodes and Peyer's patches. Immunol. Rev 2003;195:81–90. [PubMed: 12969312]
30. Gunn MD, Tangemann K, Tam C, Cyster JG, Rosen SD, Williams LT. A chemokine expressed in lymphoid high endothelial venules promotes the adhesion and chemotaxis of naive T lymphocytes. Proc. Natl. Acad. Sci. U.S.A 1998;95:258–263. [PubMed: 9419363]

31. Browning JL, Allaire N, Ngam-Ek A, Notidis E, Hunt J, Perrin S, Fava RA. Lymphotoxin-beta receptor signaling is required for the homeostatic control of HEV differentiation and function. Immunity 2005;23:539–550. [PubMed: 16286021]
32. Carragher D, Johal R, Button A, White A, Eliopoulos A, Jenkinson E, Anderson G, Caamaño J. A stroma-derived defect in NF-kappaB2$^{-/-}$ mice causes impaired lymph node development and lymphocyte recruitment. J. Immunol 2004;173:2271–2279. [PubMed: 15294939]
33. Weih F, Caamaño J. Regulation of secondary lymphoid organ development by the nuclear factor-kappaB signal transduction pathway. Immunol. Rev 2003;195:91–105. [PubMed: 12969313]
34. Lo JC, Basak S, James ES, Quiambo RS, Kinsella MC, Alegre ML, Weih F, Franzoso G, Hoffmann A, Fu YX. Coordination between NF-kappaB family members p50 and p52 is essential for mediating LTbetaR signals in the development and organization of secondary lymphoid tissues. Blood 2006;107:1048–1055. [PubMed: 16195333]
35. Moyron-Quiroz JE, Rangel-Moreno J, Kusser K, Hartson L, Sprague F, Goodrich S, Woodland DL, Lund FE, Randall TD. Role of inducible bronchus associated lymphoid tissue (iBALT) in respiratory immunity. Nat. Med 2004;10:927–934. [PubMed: 15311275]
36. van de Pavert SA, Olivier BJ, Goverse G, Vondenhoff MF, Greuter M, Beke P, Kusser K, Höpken UE, Lipp M, Niederreither K, et al. Chemokine CXCL13 is essential for lymph node initiation and is induced by retinoic acid and neuronal stimulation. Nat. Immunol 2009;10:1193–1199. [PubMed: 19783990]
37. Kim D, Mebius RE, MacMicking JD, Jung S, Cupedo T, Castellanos Y, Rho J, Wong BR, Josien R, Kim N, et al. Regulation of peripheral lymph node genesis by the tumor necrosis factor family member TRANCE. J. Exp. Med 2000;192:1467–1478. [PubMed: 11085748]
38. Yoshida H, Naito A, Inoue J, Satoh M, Santee-Cooper SM, Ware CF, Togawa A, Nishikawa S, Nishikawa S. Different cytokines induce surface lymphotoxin-alphabeta on IL-7 receptor-alpha cells that differentially engender lymph nodes and Peyer's patches. Immunity 2002;17:823–833. [PubMed: 12479827]
39. Coles MC, Veiga-Fernandes H, Foster KE, Norton T, Pagakis SN, Seddon B, Kioussis D. Role of T and NK cells and IL7/IL7r interactions during neonatal maturation of lymph nodes. Proc. Natl. Acad. Sci. U.S.A 2006;103:13457–13462. [PubMed: 16938836]
40. Mueller SN, Ahmed R. Lymphoid stroma in the initiation and control of immune responses. Immunol. Rev 2008;224:284–294. [PubMed: 18759934]
41. Mueller SN, Germain RN. Stromal cell contributions to the homeostasis and functionality of the immune system. Nat. Rev. Immunol 2009;9:618–629. [PubMed: 19644499]
42. Katakai T, Hara T, Sugai M, Gonda H, Shimizu A. Lymph node fibroblastic reticular cells construct the stromal reticulum via contact with lymphocytes. J. Exp. Med 2004;200:783–795. [PubMed: 15381731]
43. Katakai T, Suto H, Sugai M, Gonda H, Togawa A, Suematsu S, Ebisuno Y, Katagiri K, Kinashi T, Shimizu A. Organizer-like reticular stromal cell layer common to adult secondary lymphoid organs. J. Immunol 2008;181:6189–6200. [PubMed: 18941209]
44. Link A, Vogt TK, Favre S, Britschgi MR, Acha-Orbea H, Hinz B, Cyster JG, Luther SA. Fibroblastic reticular cells in lymph nodes regulate the homeostasis of naive T cells. Nat. Immunol 2007;8:1255–1265. [PubMed: 17893676]
45. Scandella E, Bolinger B, Lattmann E, Miller S, Favre S, Littman DR, Finke D, Luther SA, Junt T, Ludewig B. Restoration of lymphoid organ integrity through the interaction of lymphoid tissue-inducer cells with stroma of the T cell zone. Nat. Immunol 2008;9:667–675. [PubMed: 18425132]
46. Veiga-Fernandes H, Coles MC, Foster KE, Patel A, Williams A, Natarajan D, Barlow A, Pachnis V, Kioussis D. Tyrosine kinase receptor RET is a key regulator of Peyer's patch organogenesis. Nature 2007;446:547–551. [PubMed: 17322904]
47. Peduto L, Dulauroy S, Lochner M, Späth GF, Morales MA, Cumano A, Eberl G. Inflammation recapitulates the ontogeny of lymphoid stromal cells. J. Immunol 2009;182:5789–5799. [PubMed: 19380827]

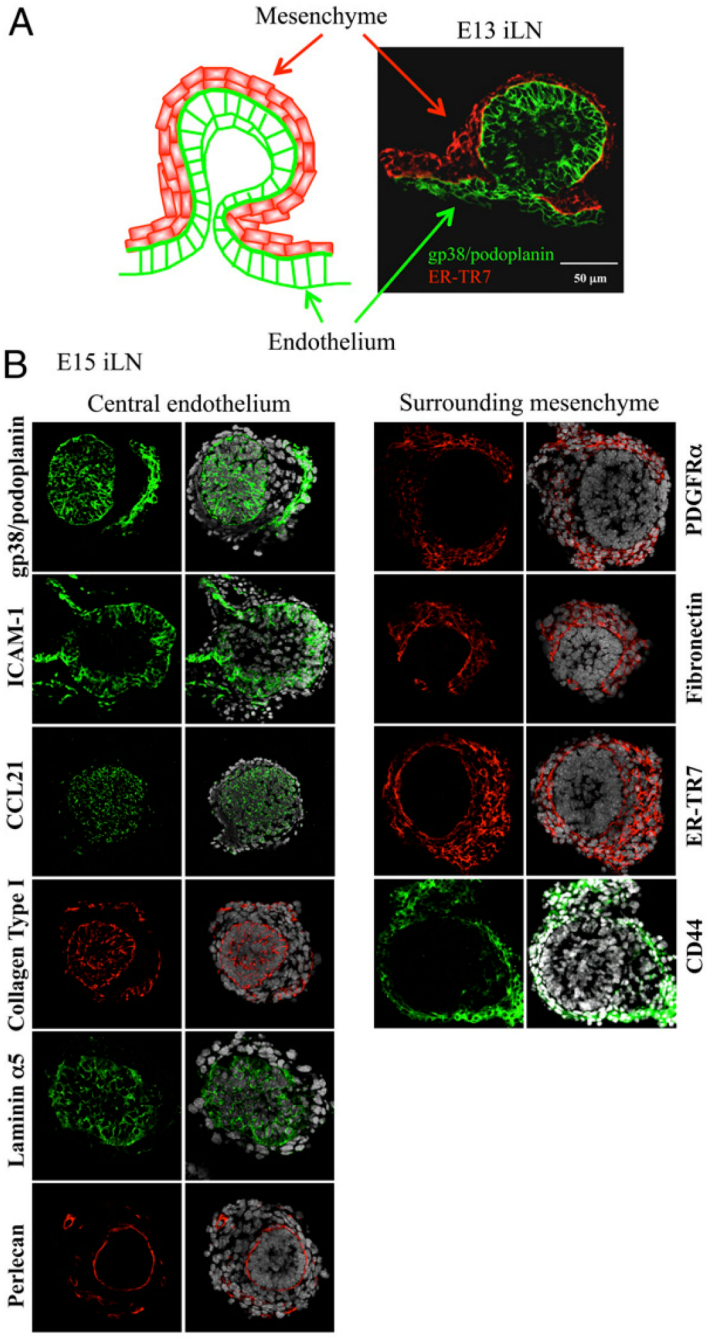

FIGURE 1.

The LN anlagen developed at the site of contact between mesenchymal and endothelial cell populations. *A*, Structure of an E13 iLN primordium. At this stage, the iLN primordium consists of a bud of endothelial cells stained with gp38/podoplanin (green) surrounded by layers of mesenchymal cells stained with ER-TR7 (red) (×40/1.4 numerical aperture [NA] water lens). *B*, Immunofluorescence staining of E15 iLN sections (×40/1.4NAwater lens) showing the central endothelium stained with gp38/ podoplanin, ICAM-1, CCL21 (green), collagen type I (red), laminin α5 (green), and perlecan (red) and the surrounding mesenchyme stained with PDGFRα, fibronectin, ER-TR7 (red), and CD44 (green). The *left panels* of all sections show the overlay with DAPI (white) staining the cell nuclei.

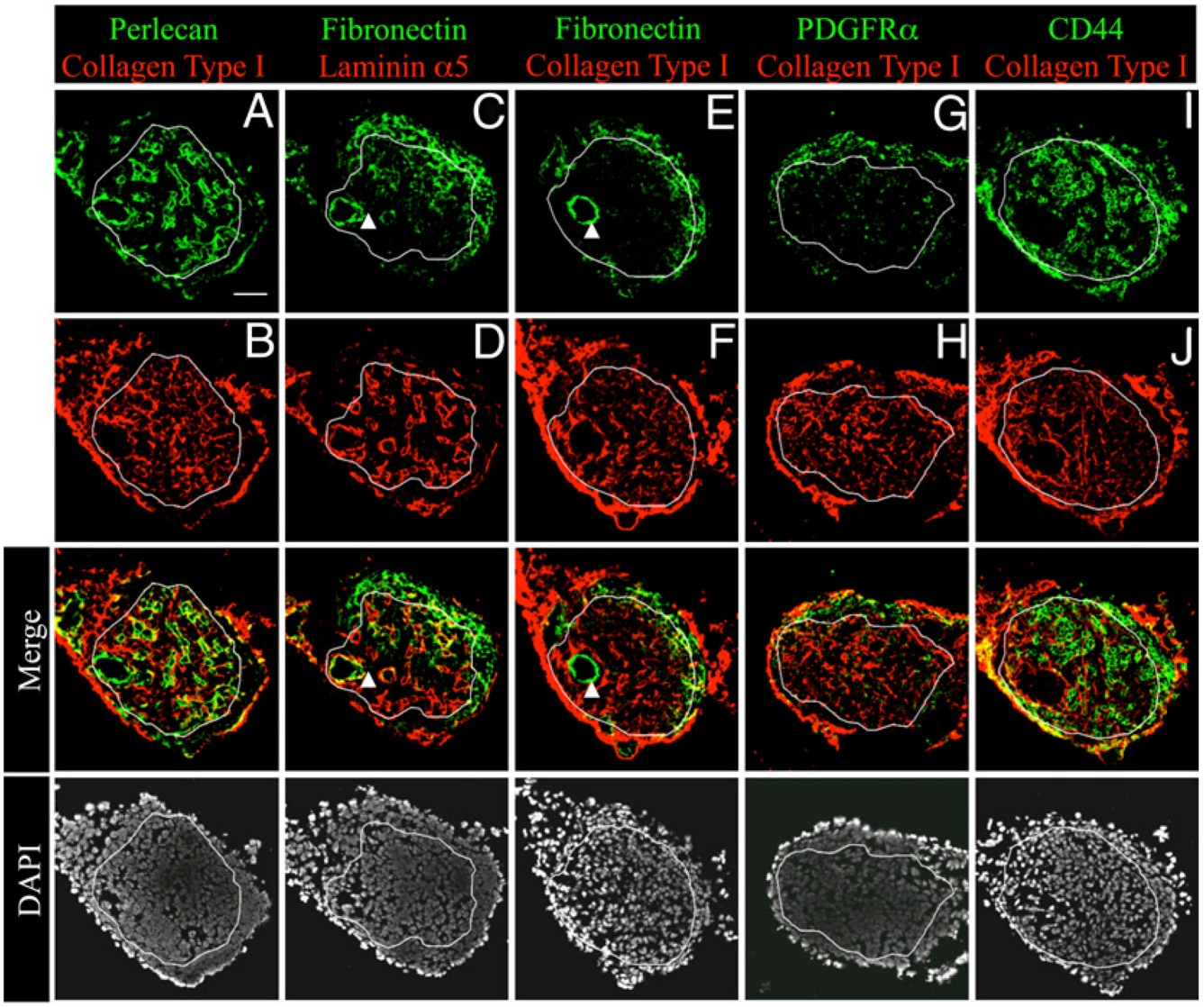

FIGURE 2.

Mesenchymal cells invade the endothelial bud around E17 in iLNs. Immunofluorescence stainings of E17 iLN sections (×25/1.4 NA water lens) showing the endothelial markers perlecan in green (*A*), collagen type I in red, (*B*, *F*, *H*, and *J*), and laminin α5 in red (*D*). The following molecules expressed by mesenchymal cells have been stained in green: PDGFRα (*G*), fibronectin (*C* and *E*), and CD44 (*I*). Note that fibronectin also stained some cells of the vasculature and CD44 also stained hematopoietic cells. A white line has been drawn encircling the endothelial cell compartment. The *bottom row* shows the DAPI (white) staining the cell nuclei. Scale bar, 50 μm (*A*).

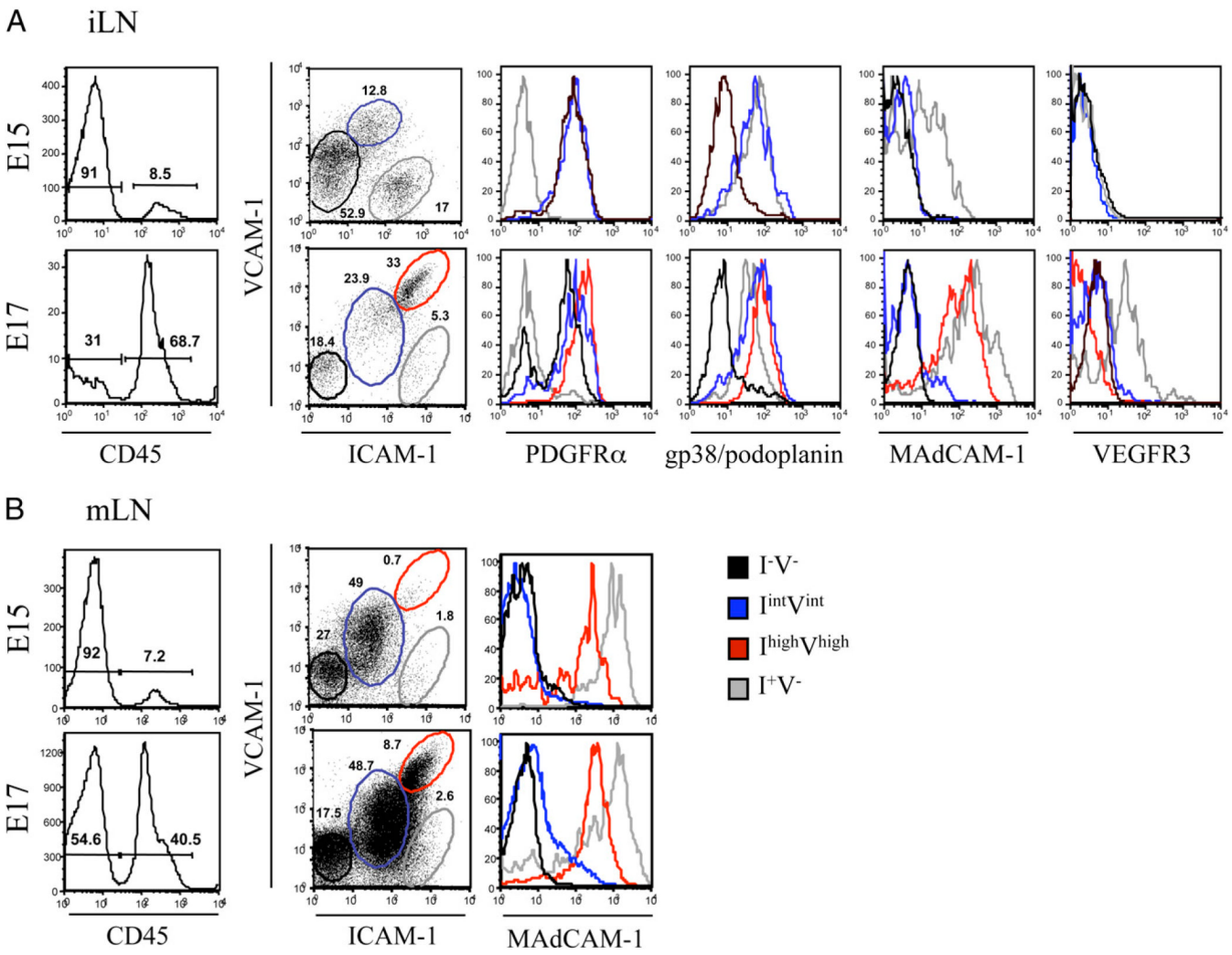

FIGURE 3.

Ontogeny of stromal organizer cells. Emergence of the $I^{high}V^{high}$ stromal organizer cells in LNs. FACS analysis of single-cell suspensions of iLN at E15 and E17 showing the recruitment of $CD45^+$ hematopoietic cells and the concomitant phenotypic changes in the $CD45^-$ stromal cells. Percentages shown in histogram correspond to $CD45^-$ stromal cells and $CD45^+$ hematopoietic cells. *A*, In iLNs, four different stromal cell populations were distinguished according to their level of expression of ICAM-1 and VCAM-1, and the levels of PDGFRα, gp38/podoplanin, MAdCAM-1, and VEGFR3 are shown for each stromal population: I^-V^- (black) expressed PDGFRα, $I^{int}V^{int}$ (blue) expressed gp38/podoplanin and PDGFRα, I^+V^- (gray) expressed gp38/podoplanin, MAdCAM-1, and VEGFR-3 (E15 and E17), and $I^{high}V^{high}$ (red) expressed PDGFRα, gp38/podoplanin, and MAdCAM-1 (E17). The ICAM-1/VCAM-1 expression profile of the $CD45^-$ cells from iLNs changed between E15 and E17 independently of whether cells were harvested and analyzed on the same day or in different days. The gates in *A* have been set up to fit according to the profile of the different ICAM and VCAM expression levels in the cell populations rather than using the same for both E15 and E17. *B*, In mLNs, the same four stromal cell populations were identified. The I^+V^- (gray) and $I^{high}V^{high}$ (red) expressed MAdCAM-1 (E15 and E17). Percentages shown in scatter plots correspond to $CD45^-$ stromal cells according to their expression of ICAM-1 and VCAM-1. Results are representative of at least three independent experiments.

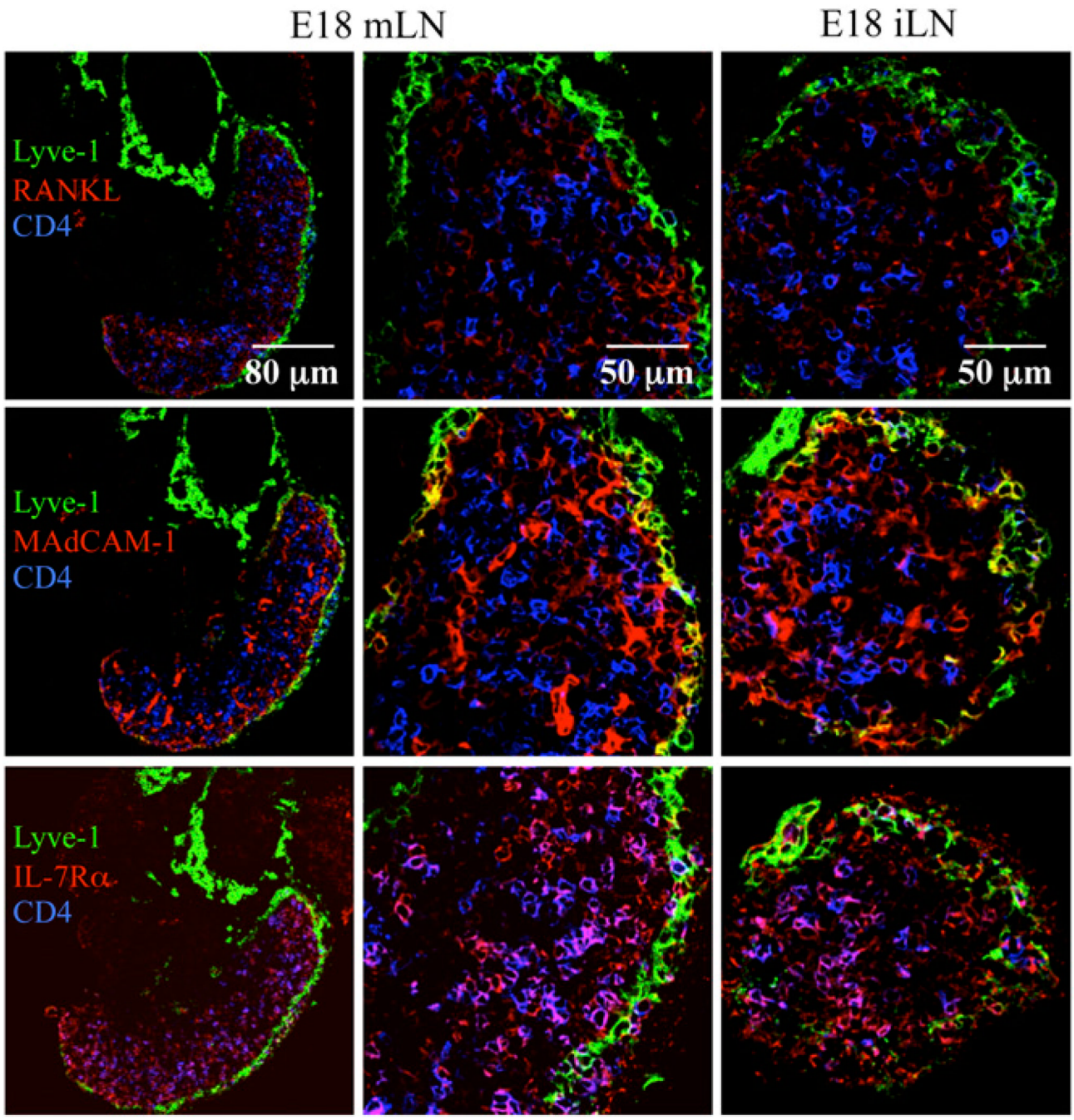

FIGURE 4.

Structures of E18 mLN and iLN. Immunofluorescence staining of E18 mLN sections (×25/1.4 NA and ×40/1.4 NA water lens) and E18 iLN sections (×40/1.4 NA water lens) showing the Lyve-1$^+$ capsule (green), the CD4$^+$ LTi cells (blue), and RANKL (top row), MAdCAM-1 (*middle row*), or IL-7Rα (*bottom row*) (red). Results are representative of at least three independent experiments.

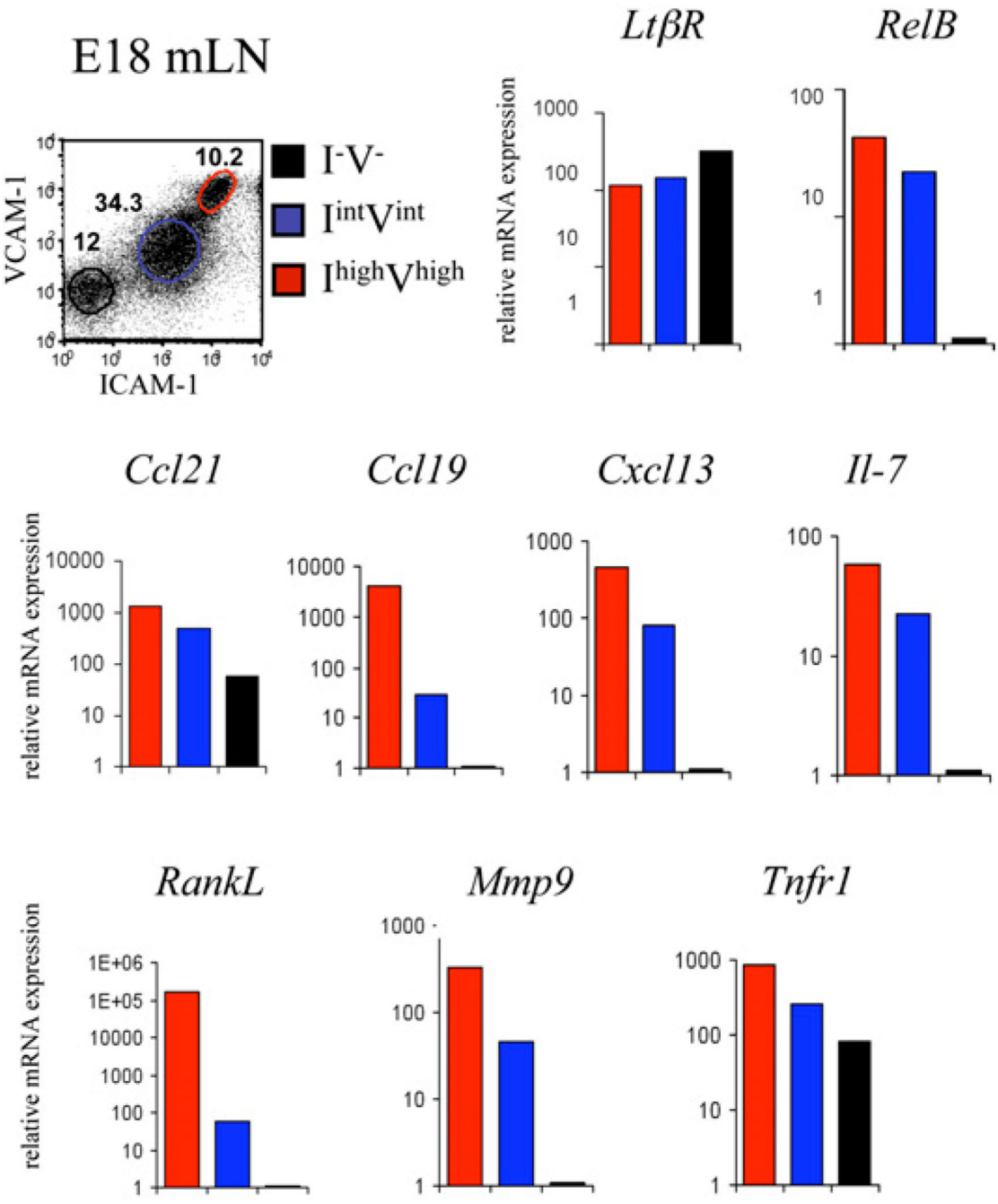

FIGURE 5.

Gradient of expression of stromal organizer markers during maturation of the mesenchyme. Cell sorting and gene expression analysis of E18 mLN $I^{-}V^{-}$ (black), $I^{low}V^{low}$ (blue), and $I^{high}V^{high}$ (red) stromal cell populations. Real-time RT-PCR analysis of *Ltβ*R, *RelB*, *Ccl21*, *Ccl19*, *Cxcl13*, *Il-7*, *RankL*, *Mmp9*, and *Tnfr1* genes. Ratio of gene of interest to β-*actin* is shown. Results are representative of at least three independent experiments.

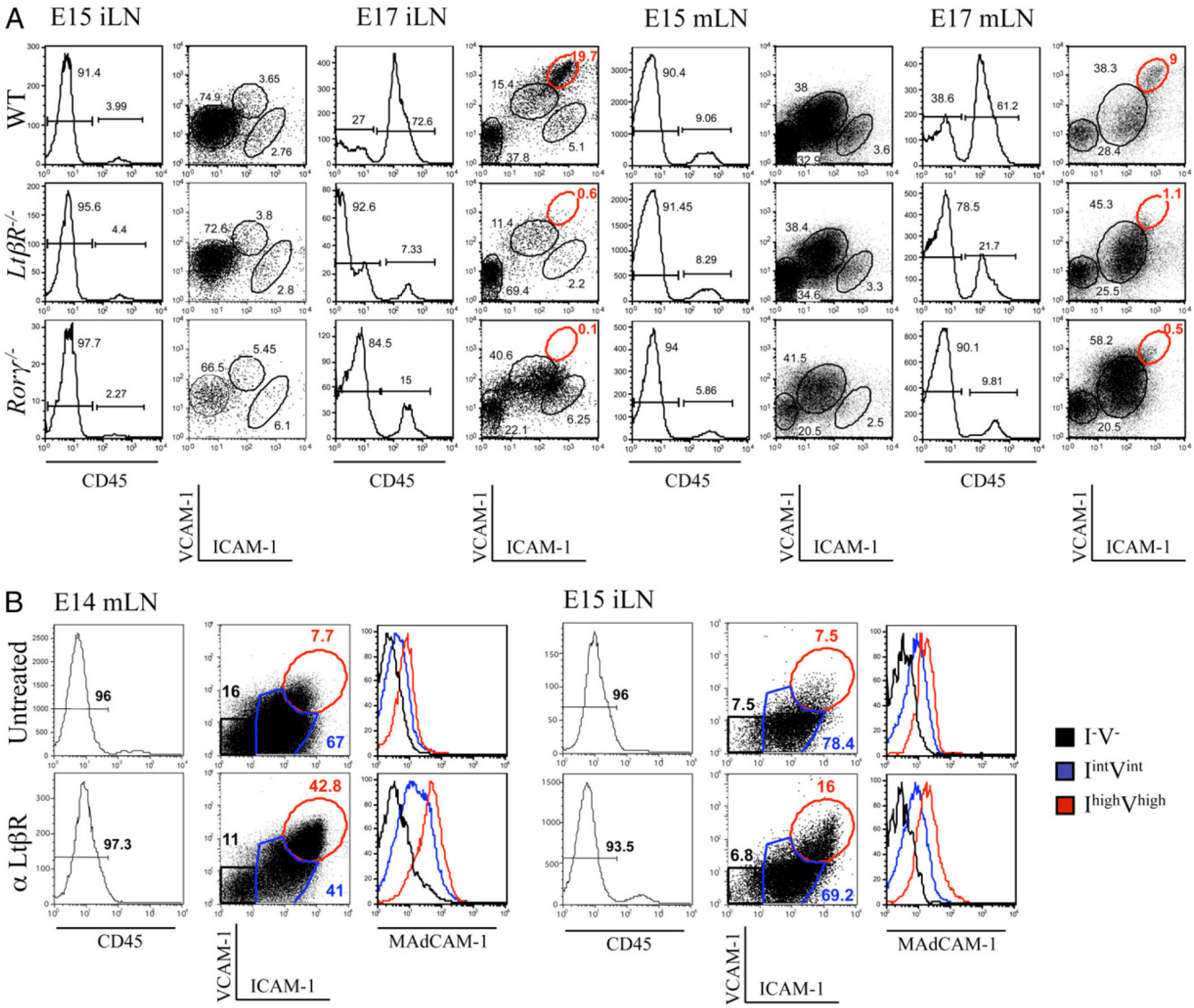

FIGURE 6.

LtβR signaling induce maturation of stromal cells from $I^{int}V^{int}$ to $I^{high}V^{high}$. *A*, FACS analysis of single-cell suspensions from WT, *Ltβ*$R^{-/-}$, and *Ror*$\gamma^{-/-}$ E15 and E17 iLNs and mLNs showing the recruitment of $CD45^+$ cells and the concomitant phenotypic changes in the $CD45^-$ stromal cells. Percentages shown in histograms correspond to $CD45^-$ stromal cells and $CD45^+$ hematopoietic cells. The different ICAM-1 and VCAM-1 $CD45^-$ stromal cell populations described in Fig. 3 are shown with corresponding percentages. Note the normal development of the *Ltβ*$R^{-/-}$ and *Ror*$\gamma^{-/-}$ E15 iLN and the absence of the $I^{high}V^{high}$ stromal cell populations in the *Ltβ*$R^{-/-}$ and *Ror*$\gamma^{-/-}$ E15 mLNs and E17 iLNs and mLNs. Results are representative of at least three independent experiments. *B*, LTβR stimulation induces the maturation of stromal cells from $I^{int}V^{int}$ to $I^{high}V^{high}$ in E14 mLN and E15 iLN organ cultures. FACS analysis of single-cell suspensions of E14 mLNs (*left panels*) and E15 iLNs (*right panels*) in organ cultures for 3 d showing the phenotypic changes in the $CD45^-$ stromal cells induced by agonistic αLTβR Ab (*bottom panels*). Percentages shown in histograms correspond to $CD45^-$ stromal cells. Three different stromal cells populations were identified: I^-V^- (black),

$I^{int}V^{int}$ (blue), and $I^{high}V^{high}$ (red). Expression levels of MAdCAM-1 for each cell population are shown in histograms. Results are representative of three independent experiments.

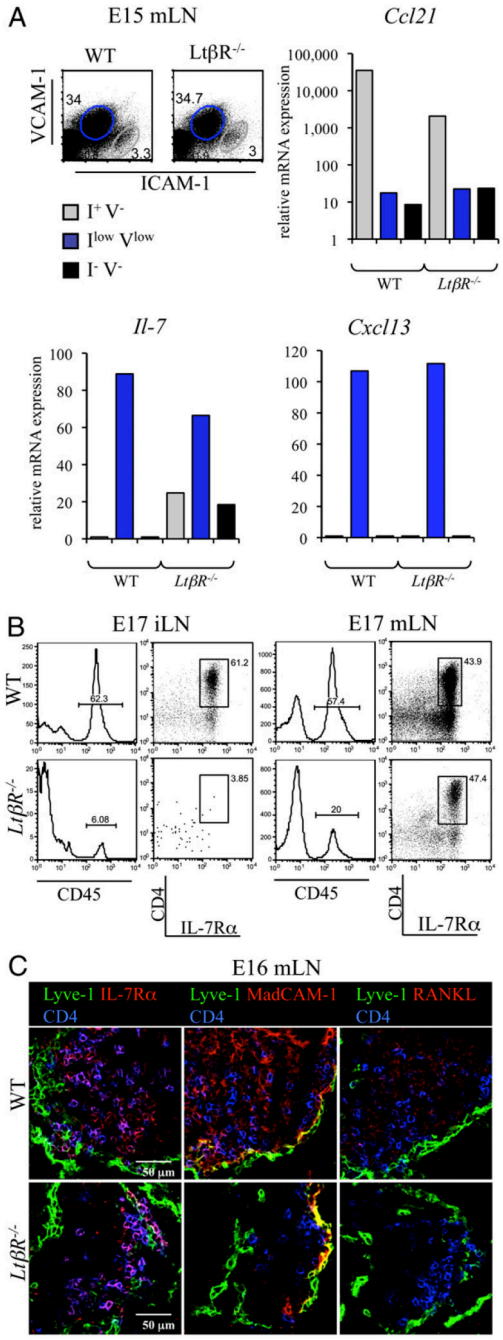

FIGURE 7.

LTβR is not fully required for the recruitment and retention of LTi cells to mesenteric LNs. *A*, Cell sorting and gene expression analysis of the WT and *LtβR*$^{-/-}$ E15 mLN I^{-}V^{-} (black), I^{int}V^{int} (blue), and I^{+}V^{-} (gray) stromal cell populations. Real-time RT-PCR analysis of the *Ccl21*, *Il-7*, and *Cxcl13* genes. Ratio of gene of interest to β-*actin* is shown. Results are representative of two independent experiments. *B*, LTβR is required for the recruitment of LTi cells to iLNs but not mLNs. FACS analysis of single-cell suspensions from WT and *LtβR*$^{-/-}$ E15 and E17 iLNs and mLNs showing the percentage of CD45^{+} cells and CD4^{+}IL-7Rα^{+} LTi cells. Percentages shown in histograms correspond to CD45^{+} hematopoietic cells. CD45^{+} hematopoietic cell dot plot analysis of CD4 and IL-7Rα showed the percentages of LTi cells.

Note the presence of LTi cells in the *Lt*β*R*$^{-/-}$ E17 mLN and their absence in iLNs. *C*, Immunofluorescence staining of WT and *Lt*β*R*$^{-/-}$ E16 mLN sections (×40/1.4 NA water lens) showing the Lyve-1^{+} capsule (green), CD4^{+} LTi cells (blue), and in red, IL-7Rα (*left panels*), MAdCAM-1 (*middle panels*), or RANKL (*right panels*). Note in the *Lt*β*R*$^{-/-}$ mLNs the presence of the capsule expressing Lyve-1 and MAdCAM-1, the presence of LTi cells coexpressing IL-7Rα and CD4, and the absence of RANKL expression. Results are representative of two independent experiments.

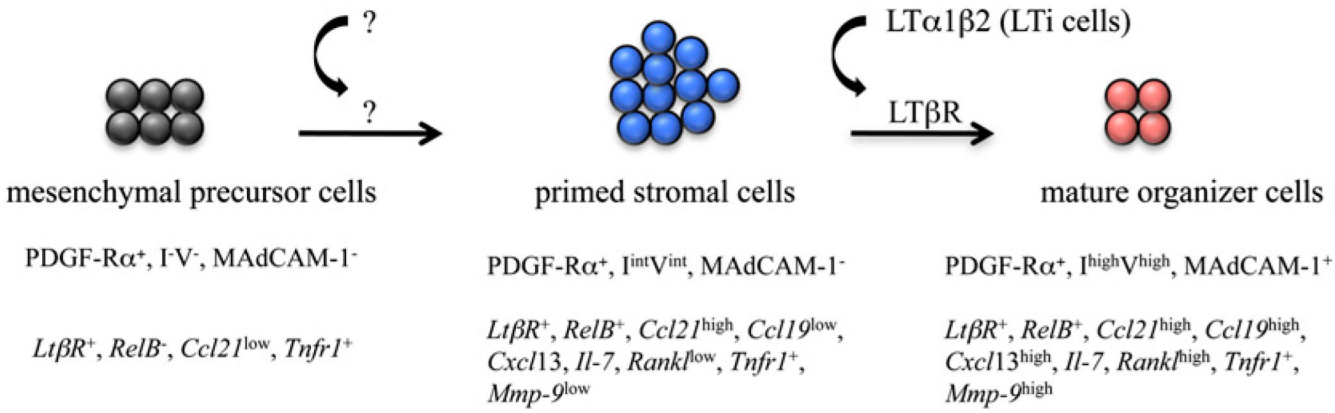

FIGURE 8.

Model of LN stromal cell maturation. Based on our immunfluorescence and FACS analysis data (summarized in the *top row* in capital letters) and qPCR data (summarized in the *bottom row* in italics), we propose a model for the maturation of stromal cells during LN development. The $I^{-}V^{-}$ mesenchymal precursor cells (dark gray), upon stimulation by an unknown signal, will become $I^{int}V^{int}$ primed stromal cells (blue) that upon upregulating the expression of RelB will be able to respond to LTβR signals upon engagement by the lymphotoxin α1β2 ligand expressed by LTi cells. Signals through the LTβR and other receptors induce the maturation of the $I^{int}V^{int}$ cells (red) to become $I^{high}V^{high}$ stromal organizer cells (see *Discussion*).